Progress In Electromagnetics Research, Vol. 113, 379–393, 2011

HALF MODE MICROWAVE FILTERS BASED ON EPSILON NEAR ZERO AND MU NEAR ZERO CONCEPTS

B. López-García, D. V. B. Murthy, and A. Corona-Chávez

Electronics Department
National Institute of Astrophysics, Optics and Electronics (I.N.A.O.E)
Puebla 72840, Mexico

Abstract—A new design of microwave band pass filter design is presented using metamaterial-inspired Epsilon Near Zero (ENZ) and Mu Near Zero (MNZ) behaviors. These filters are based on waveguide technology. The proposed structure allows us to reduce the number of tunnels normally used for passband filter design by reducing its size. It is also incorporated the half mode concept to the tunnels leading a greater miniaturization. Two Chebyshev filters with two and four-poles were designed, fabricated and measured showing good agreement between simulated and experimental results.

1. INTRODUCTION

The use of metamaterials in several fields has recently marked considerable interest in the scientific community due to their exotic electromagnetic properties (i.e., negative, very small or very large permittivity and permeability) and potential utilities [1–4]. Among these special material properties, near zero permittivity (also called Epsilon Near Zero) [5–9], and near zero permeability (known as Mu Near Zero) [10–12], have attracted much attention due to their potential applications at microwave frequencies.

One of such potential applications is the capability of miniaturization as demonstrated in previous works such as Tassin et al. [13], who performed an optical waveguide structure with a left-handed material layer to reduce its thickness below the wavelength of light. This design allows for good light confinement in a subwavelength thin waveguide, and thereby leading to miniaturization. Oulton et al. [14], proposed

Received 7 October 2010, Accepted 9 February 2011, Scheduled 10 February 2011
Corresponding author: Benjamin Lopez-Garcia (benjamin_lopez@ieee.org).

a design that integrates dielectric waveguides with plasmonics. Such design consists of a dielectric nanowire separated from a metal surface by a nanoscale dielectric gap, in which can be supported an effective subwavelength transmission.

In this paper, a new method for microwave filter design based on metamaterial-inspired Epsilon Near Zero (ENZ) and Mu Near Zero (MNZ) concepts is presented. This design starts by designing a short Epsilon Near Zero tunnel at a given frequency [5]. Subsequently, this tunnel is loaded with an interdigital capacitor that forces the effective permeability to have a frequency dispersive behavior [10, 11]. The equivalent circuit is a Composite Right Left Handed (CRLH) unit cell [15–20], with a step feed. By making this unit cell unbalanced [17], two tunneling frequencies are excited at the points where the effective permittivity and permeability are zero, making the propagation constant also zero ($\beta = 0$) at such frequencies. The equivalent behavior of this unit cell is similar to a dual mode resonator [3]. Moreover, this unit cell must be much smaller than quarter wavelength to comply with the homogeneity condition [7].

Finally, in order to miniaturize the circuit, the cell is split to half by incorporating the half mode concept [21], which has been applied to the design of several microwave devices [22–25].

As demonstrated in [5, 6], to achieve Epsilon Near Zero behavior, waveguide technology is implemented, where a rectangular waveguide filled with a relative permittivity ε_r presents an effective permittivity with a dispersive behavior when operated at the fundamental TE_{10} mode as shown in Equation (1)

$$\frac{\varepsilon_{eff}}{\varepsilon_o \varepsilon_r} = n^2 - \frac{c^2}{4\varepsilon_r f^2 W_t^2} \tag{1}$$

where ε_r is the relative permittivity of the material, n is the refractive index of the filling material, c is the speed of light in vacuum, W_t is the waveguide width in the H-plane, and f is the operation frequency. As observed from this equation, at cutoff frequency, the effective permittivity (ε_{eff}) is approximately zero and therefore the propagation constant is zero ($\beta = 0$). It is also observed that when $\varepsilon_{eff} \sim 0$ the signal follows a static-like behavior that allows reflectionless propagation. Due to this static-like behavior of the fields in Epsilon Near Zero behavior, it may be possible to squeeze and tunnel electromagnetic energy through a very narrow Epsilon Near Zero tunnel [8, 9]. Moreover, the energy can be tunneled at a particular frequency independently of the tunnel's total length, which leads to considerable miniaturization.

The width of the Epsilon Near Zero tunneling waveguide operating

at TE_{10} mode is given by Equation (2)

$$W_p = \frac{c}{2f_0\sqrt{\varepsilon_r}} \tag{2}$$

where f_o is the tunneling frequency, c is the speed of light, and ε_r is the relative permittivity.

In order to have tunneling, a very abrupt discontinuity between the waveguide and the tunnel must exist to ensure that only signals around the Epsilon Near Zero frequency are tunneled through, while others are reflected back. Hence the waveguide height h_s should be much larger than the tunnel height h_t as shown in Figure 1.

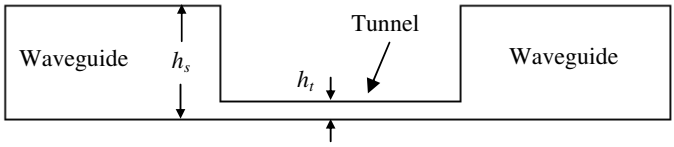

Figure 1. Schematic of the Epsilon Near Zero approach using waveguide technology.

Mu Near Zero structure is a metamaterial whose behavior presents a frequency dispersive effective-permeability that can become zero at a particular frequency. If a metamaterial presents a behavior such that $\mathrm{Re}[\mu(\omega_c)] \approx 0$ and $\mathrm{Im}[\mu(\omega_c)]$ be small, for a small range of frequency around the cutoff frequency $f = \omega_c/2\pi$, a situation of a medium with zero permeability can be reached [10]. Several designs have been proposed in the literature, whose properties can be improved by using Mu Near Zero behavior. Jin et al. [11] explained the electromagnetic energy squeezing mechanism by using a Mu Near Zero structure which consists of a dielectric split ring with opened gap. Yang et al. [12] proposed a high directive slab antenna using a Mu Near Zero/Epsion Near Zero metamaterial slab and an embedded line source. Caloz and Itoh [18], provide a method to realize an artificial lumped-element LH transmission line and propose a microstrip implementation of this line through a series interdigital capacitor and a shorted stub inductor. Dong and Itoh [20] obtain Mu Near Zero behavior by adding a series capacitance to a rectangular waveguide propagating the TE_{10} mode.

In this work, a waveguide resonator is proposed where Epsilon Near Zero and Mu Near Zero phenomena are present. By designing Epsilon Near Zero and Mu Near Zero at the appropriate frequencies, the overall performance of the proposed circuit is similar to a dual mode resonator. Moreover, this circuit is utilized to realize two and four pole Chebyshev filters.

2. DESIGN OF EPSILON NEAR ZERO — MU NEAR ZERO STRUCTURE

2.1. Epsilon Near Zero Tunnel

The circuit starts by designing an Epsilon Near Zero tunnel, using a substrate with permittivity of $\varepsilon_r = 2.2$ and height $h_s = 1.57\,\text{mm}$. According to the previous section, in order to tunnel a single frequency, the condition $h_s \gg h_t$ must be satisfied [6]. Thus, a tunnel height $h_t = 0.4\,\text{mm}$ was chosen. The tunnel width at the frequency of operation of 2.5 GHz was calculated according to Equation (2) providing a tunnel width of $W_p = 40.5\,\text{mm}$. The tunnel length $L_t = 10\,\text{mm}$ was optimized through several simulations using a Full-Wave Electromagnetic Field Simulator [26]. As explained in previous section, the energy transmitted through the tunnel is independent of its length and therefore, the final value of L_t was comfortably chosen such that the Fabry-Perot resonance (5.36 GHz) will appear out of the frequency band of interest (2.5–2.8 GHz). The material modeled was a substrate Rogers RT/duroid 5880 with permittivity of $\varepsilon_r = 2.2$ and for all metal layers copper material with a conductivity of $\sigma = 58 \times 10^6\,\text{S/m}$ was used. The response in frequency of the simulated tunnel is shown in Figure 2(a). The effective medium permittivity ε_{eff} and dispersion diagram β are extracted from simulated S-parameters of tunnel's structure following the procedure mentioned in [27]. The variation of ε_{eff} and β (per unit cell length L_{total}) with frequency are shown in Figures 2(b) and 2(c), respectively, showing the Epsilon Near Zero behavior at the resonance frequency. The total dimensions of the tunnel are shown in Figure 3(a).

Once the Epsilon Near Zero tunnel was designed, the half mode concept was applied into it. As shown in [21], if a magnetic wall is

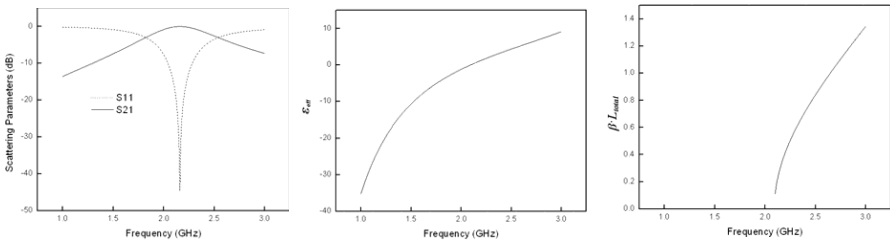

(a) (b) (c)

Figure 2. (a) Response in frequency of scattering parameters, (b) effective permittivity ε_{eff}, and (c) dispersion diagram β per unit cell length L_{total} of the Epsilon Near Zero tunnel.

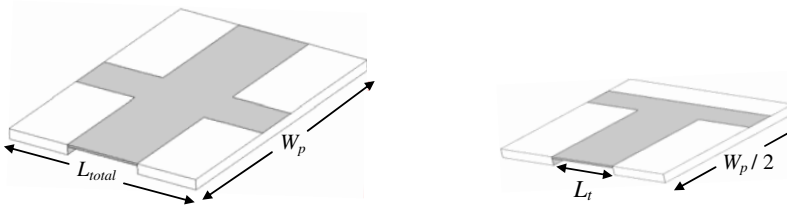

Figure 3. Schematic of the Epsilon Near Zero tunnel structure in (a) complete-mode and (b) half-mode configurations. The total dimensions of the tunnel are $W_p = 40.5\,\text{mm}$ by $L_{total} = 32\,\text{mm}$.

applied to a waveguide propagating the TE_{10} mode along the line of the propagation direction, the field distribution is unchanged. Therefore the tunnel can be cut into half as shown in Figure 3(b). Then the final width is $W_p/2 = 20.25\,\text{mm}$.

2.2. Mu Near Zero Behavior

The introduction of the interdigital capacitor into the Epsilon Near Zero tunnel results in creating a frequency dispersive behavior of the equivalent permeability. As shown in [20], the equivalent circuit of this structure is a Composite Right Left Handed unit cell. If this unit cell is designed for an unbalanced case, the Epsilon Near Zero and Mu Near Zero phenomena will occur at different frequencies. Thus, several simulations using unbalanced configuration were carried out with different number of fingers (n), finger widths (W_f), and finger-separation widths (W_{sep}), to achieve the best performance in bandwidth. Only the capacitor length L_c was chosen according to the desired external coupling Q_e, as will be discussed in Section 3. The final dimensions of the interdigital capacitor were calculated to have an Mu Near Zero tunneling frequency of 2.8 GHz, which are: $W_f = 0.35\,\text{mm}$, $W_{sep} = 0.30\,\text{mm}$, and $n = 10.5$, as shown in Figure 4. Figure 4 also shows the final half mode tunnel structure, while Figure 5 depicts the effective parameter μ_{eff} extracted using the procedure shown in [27], which clearly presents a Mu Near Zero behavior at the frequency of 2.8 GHz.

The equivalent circuit of the half-mode tunnel with interdigital capacitor when $W_m = W_{m1}$ is shown in Figure 6(a). Moreover, since the condition to have the tunneling effect is that $h_t \ll h_s$, this discontinuity can be modeled as shunt susceptance B as shown in [28]. The interdigital capacitor is included in the model as

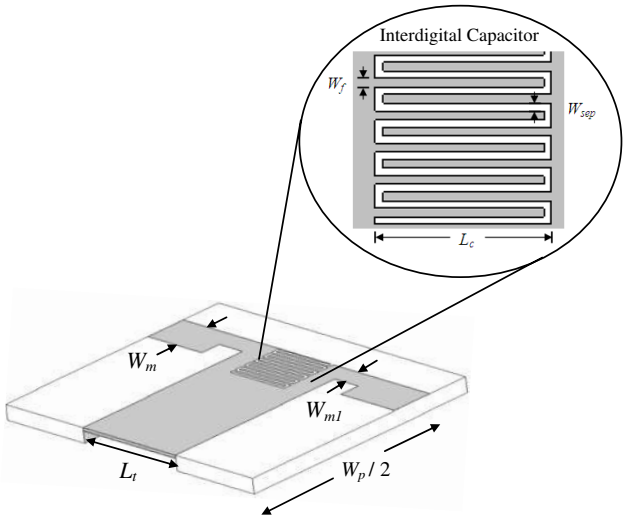

Figure 4. Schematic of the Epsilon Near Zero — Mu Near Zero half-mode tunnel structure.

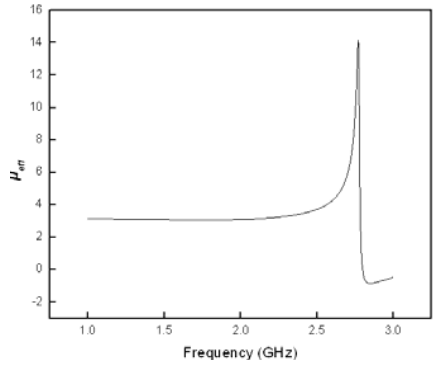

Figure 5. Effective parameter μ_{eff} of the half-mode Epsilon Near Zero tunnel structure with interdigital capacitor.

C_L, while L_L represents the inductance produced by the via wall. The shunt capacitance C_R and the series inductance L_R correspond to the parasitic capacitance from the fingers and the distributed series inductance from the waveguide, respectively [20]. Waveguide discontinuity in height is also included in the model as capacitor C_B [28]. The component values of the Composite Right Left Handed unit cell are $C_L = 0.2470\,\text{pF}$, $L_L = 42.137\,\text{nH}$, $C_R = 0.7410\,\text{pF}$, and $L_R = 30.168\,\text{nH}$ [17]. A simulation was carried out using these values

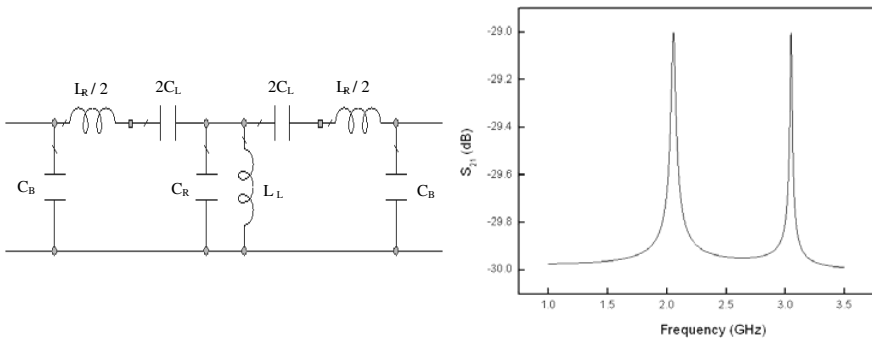

(a) (b)

Figure 6. (a) Equivalent circuit and (b) response in frequency of the transmission coefficient S_{21} of the half-mode Epsilon Near Zero — Mu Near Zero tunnel.

Table 1. Specifications of two-pole and four-pole filter.

Two-pole Filter	Four-pole Filter
$g_0 = 1$	$g_0 = 1$
$g_1 = 0.4283$	$g_1 = 0.7128$
$g_2 = 0.4283$	$g_2 = 1.2003$
$g_3 = 1.1$	$g_3 = 1.3212$
	$g_4 = 0.6476$
	$g_3 = 1.1007$
$FBW = 7\%$	$FBW = 10\%$
$k = 0.13$	$k = 0.11$
$Q = 6.14$	$Q = 10.18$

and keeping C_B very large to account for the large step-discontinuity. The results are shown in Figure 6(b), where it is clear that only two frequencies propagate, which are those at which ε_{eff} and μ_{eff} are equal to zero, corresponding to 2.5 GHz and 2.8 GHz from Figures 2(b) and 5.

3. FILTER DESIGN

Two filters, a two pole and a four pole with Chebyshev responses were designed with the Epsilon Near Zero — Mu Near Zero structure described above.

A two-pole filter was designed at the central frequency f_0 =

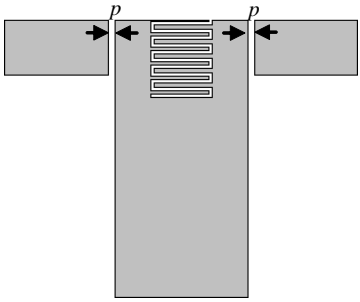

Figure 7. Tunnel structure used to calculate the coupling k factor. The capacitive gap used was $p = 0.1$ mm.

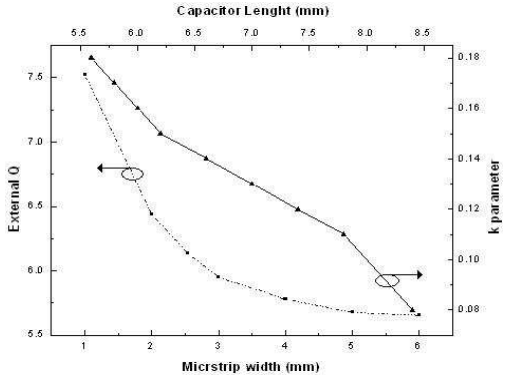

Figure 8. Graphs of the k parameter vs. capacitor length L_c and the external quality factor Q_e vs. microstrip width W_{m1}.

2.5 GHz and a fractional bandwidth $FBW = 7\%$. This filter comprises of one unbalanced unit cell with Epsilon Near Zero and Mu Near Zero tunneling frequencies. The g parameters are obtained from [29] for a 0.01 dB ripple which are shown in Table 1. Then the external coupling Q_e and the resonator coupling k are obtained from Equations (3) and (4), respectively, as $Q_e = 6.14$ and $k = 0.13$.

$$Q_e = \frac{g_0 \cdot g_1}{FBW} \tag{3}$$

$$k = \frac{FBW}{\sqrt{g_1 \cdot g_2}} \tag{4}$$

To calculate the coupling coefficient k, full wave simulations are carried out using the structure shown in Figure 7, where the capacitor loaded tunnel is weakly coupled to the feed lines through a capacitive gap p. The coupling coefficient k depends on the length L_c of the interdigital capacitor, which was varied in a range from 5.6 mm to 8.4 mm. It is noted that by changing L_c the Mu Near Zero frequency is changed, whereas Epsilon Near Zero is fixed.

For these calculations two microstrip lines weakly coupled through a capacitive gap $p = 0.1$ mm were used. The k value was extracted from Equation (5) [29].

$$k = \frac{f_2^2 - f_1^2}{f_2^2 + f_1^2} \tag{5}$$

where f_1 and f_2 are the corresponding resonant frequencies obtained

from the simulated results. Figure 8 illustrates the plot of the obtained k values versus the different capacitor lengths.

To calculate the external coupling Q_e, full wave simulations are also carried out. The external coupling depends on the width of the microstrip line W_{m1}, which was varied in a range from 1 mm to 6 mm. For these calculations the interdigital capacitor was not included and one side of the tunnel was weakly coupled with a gap $p = 0.6$ mm, as shown in Figure 9. The external coupling was obtained from Equation (6) [29].

$$Q_e = \frac{f_0}{FBW} \tag{6}$$

Figure 8 plots the different external quality factors versus the width of the microstrip line W_{m1}.

The filter was implemented and fine-tuned in [26] with the dimensions calculated from Figure 8. The final dimensions of the two-pole filter are: $h_s = 1.57$ mm, $h_t = 0.4$ mm, $L_t = 10$ mm, $L_c = 7$ mm, $W_m = 5$ mm, and $W_{m1} = 2.54$ mm.

In order to implement a four-pole filter, two Epsilon Near Zero — Mu Near Zero unit cells are utilized. The characteristics of the filter are a fractional bandwidth $FBW = 10\%$ with 0.01 dB ripple. The low pass element g parameters are also taken from [27]. The external coupling and the coupling $k_{i,i+1}$ factors are obtained as $Q_e = 7.13$, $k_{1,2} = k_{3,4} = 0.11$, $k_{2,3} = 0.08$, from Equations (3) and (7), respectively.

$$k_{i,i+1} = \frac{FBW}{\sqrt{g_i \cdot g_{i+1}}}, \text{ for } i = 1 \text{ to } n-1 \tag{7}$$

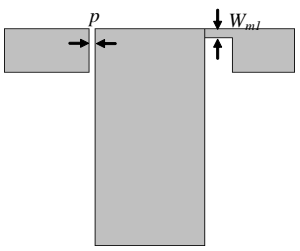

Figure 9. Tunnel structure used to calculate Q_e.

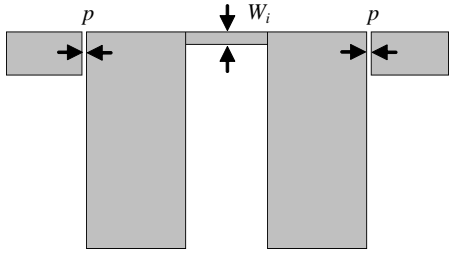

Figure 10. Epsilon Near Zero structure implemented to calculate the coupling $k_{2,3}$ between contiguous Epsilon Near Zero — Mu Near Zero unit cells.

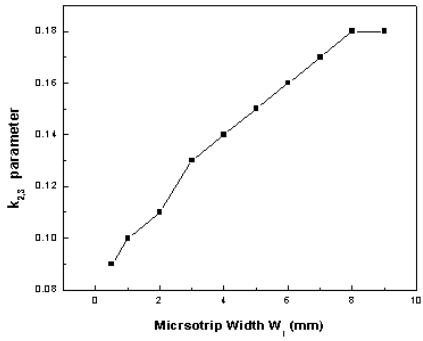

Figure 11. Graph of $k_{2,3}$ factor vs. microstrip width W_i.

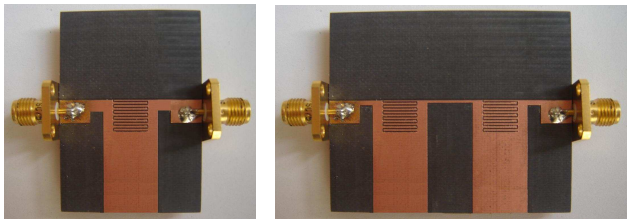

Figure 12. Photographs of the constructed (a) two-pole and (b) four-pole Epsilon Near Zero — Mu Near Zero filters.

where n is the number of poles. Specifications of both filters are presented in Table 1.

To calculate the coupling $k_{2,3}$ between contiguous tunnels, the structure in Figure 10 was simulated in [26]. The width W_i of the microstrip line between tunnels was varied from 0.5 mm to 9 mm. External microstrip lines were weakly coupled through a capacitive gap $p = 0.2$ mm and used for calculations. Figure 11 plots the different widths vs. the corresponding values of coupling factor $k_{2,3}$.

The filter was also fine tuned in the simulator [26]. The final layout dimensions are: $h_s = 1.57$ mm, $h_t = 0.4$ mm, $L_t = 10$ mm, $L_c = 7.8$ mm, $W_m = 5$ mm, $W_{m1} = 1.0$ mm, and $W_i = 0.5$ mm.

4. EXPERIMENTAL RESULTS

Two-pole and four-pole filters were fabricated with a standard PCB milling machine and all the layers were properly metalized. The substrate used to fabricate the circuits was *RT Duroid 5880* with $\varepsilon_r = 2.2$ and substrate height $h_s = 1.57$ mm. The height of the tunnel

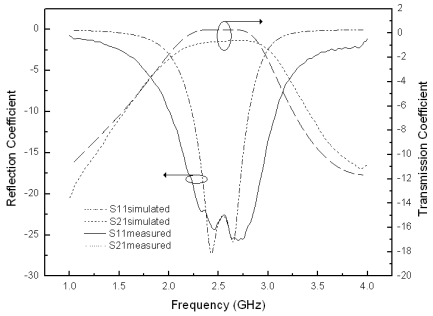

Figure 13. Simulated and experimental responses of two-pole half-mode Epsilon Near Zero — Mu Near Zero filter.

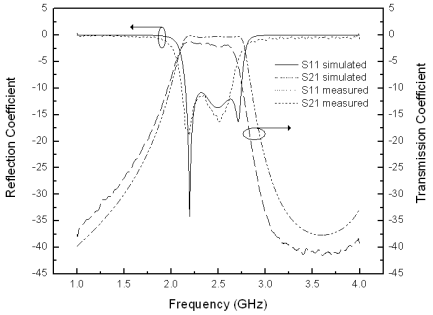

Figure 14. Simulated and experimental responses of four-pole half-mode Epsilon Near Zero — Mu Near Zero filter.

is $h_t = 0.4\,\text{mm}$ and its length $L_t = 10\,\text{mm}$. In order to measure their response, standard SMA connectors were placed at the input and output lines of both filters. Photographs of the fabricated filters are shown in Figure 12.

The physical dimensions for the two-pole and four pole filters are $32 \times 30\,\text{mm}^2$ and $54 \times 30\,\text{mm}^2$ respectively. These dimensions are smaller, if we compare, for example, the two-pole filter with other earlier works such as Liu and Huang [30], who proposed a SIW band-pass filter at central frequency of 5.8 GHz and physical size of $99.2 \times 49.6\,\text{mm}^2$. Deng [31] proposed a coplanar stripline bandpass filter with a bandwidth from 4.15 to and Yu [32] developed circular waveguide resonators for filter applications with a bandwidth from 11 to 11.25 GHz, and a physical size of 20.244 mm in diameter and minimum length of 31.4 mm. Using our design for a two-pole filter at frequencies of 5 GHz and 11 GHz, dimensions of approximately $10.1 \times 6.1\,\text{mm}^2$ and $4.6 \times 3.3\,\text{mm}^2$ can be reached, respectively.

The filter characteristics were measured using a PNA series microwave Vector Network Analyzer (E8361A, *Agilent*). The responses of the fabricated and simulated two-pole and four-pole filters are shown in Figures 13 and 14, respectively. The experimental and simulated center frequency for both filters is 2.5 GHz. In the two-pole case the return losses all over the band are about $-17\,\text{dB}$ and $-23\,\text{dB}$ for the experimental and simulated filters, respectively. The simulated insertion losses are about 0.4 dB and the experimental about 1.8 dB.

In the four-pole filter the return losses throughout the band are below 10 dB for the experimental and simulated filters. The insertion losses are about 0.04 dB and about 0.5 dB, for the experimental and

simulated filters, respectively.

The responses of both filters present very good agreement between the experimental and simulated results, showing the viability of the method. The small variations between them are due to fabrication errors and material tolerances.

5. CONCLUSION

A novel method for the design of highly miniaturized microwave filters using Epsilon Near Zero — Mu Near Zero behaviors in waveguide technology was presented. Adding the interdigital capacitor to the Epsilon Near Zero tunnel allows us to reduce the number of resonators normally used for passband filter design. In addition, the use of the half mode concept to the proposed structure leads us to a greater miniaturization in comparison with traditional filters. Even more this new methodology can be easily integrated with other planar devices, such as antennas, mixers, amplifiers, etc., which are widely used for communication, radar and image reconstruction systems. Finally to probe the feasibility of this new methodology two-pole and four-pole filters were successfully designed and fabricated, showing good agreement between simulated and experimental results.

REFERENCES

1. Hwang, R. B. H. W. Liu, and C.Y. Chin, "A metamaterial-based *E*-plane horn antenna," *Progress In Electromagnetics Research*, Vol. 93, 275–289, 2009.
2. Gong, Y. and G. Wang, "Superficial tumor hyperthermia with flat left-handed metamaterial lens," *Progress In Electromagnetics Research*, Vol. 98, 389–405, 2009.
3. Jang, G. and S. Kahng, "Design of a dual-band metamaterial band-pass filter using zeroth order resonance," *Progress In Electromagntics Research C*, Vol. 12, 149–162, 2010.
4. Navarro-Cía, M., J. M. Carrasco, M. Beruete, and F. Falcone, "Ultra-wideband metamaterial filter based on electroinductive-wave coupling between microstrips," *Progress In Electromagnetics Research Letters*, Vol. 12, 141–150, 2009.
5. Alù, A., M. G. Silveirinha, A. Salandrinoz, and N. Engheta, "Epsilon-near-zero (ENZ) metamaterials and electromagnetic sources: Tailoring the radiation phase pattern," *Phys. Rev. B*, Vol. 75, No. 15, 155410, 2007.

6. Murthy, D. V. B., A. Corona-Chávez, and J. L. Olvera-Cervantes, "A novel epsilon near zero (ENZ) tunneling circuit using microstrip technology for high integrability applications," *Progress In Electromagnetics Research C*, Vol. 15, 65–74, 2010.
7. Edwards, B., A. Alù, M. G. Silveirinha, and N. Engheta1, "Reflectionless sharp bends and corners using epsilon-near-zero effects," *Journal of Applied Physics*, Vol. 105, No. 4, 044905, 2009.
8. Edwards, B., A. Alù, M. G. Silveirinha, and N. Engheta, "Comparison between ε-near-zero and fabry-perot resonant transmission through waveguide bends and channels," *URSI General Assembly*, 303, Chicago, IL, USA, Aug. 2008.
9. Edwars, B., A. Alù, M. E. Young, M. Silveirinha, and N. Engheta, "Experimental verification of epsilon-near-zero metamaterial coupling and energy squeezing using a microwave waveguide," *Physical Review Letters*, Vol. 100, No. 3, Jan. 2008.
10. Garcia, N., M. Munoz, E. V. Ponizovskaya, and M. Nieto-Vesperinas, "Zero permeability materials (ZmuM): A way out of the left handed materials trap," Cornell University Library, 2002.
11. Jin, Y., P. Zhang, and S. He, "Squeezing electromagnetic energy with a dielectric split ring inside a permeability-near-zero metamaterial," *Phys. Rev. B*, Vol. 81, 085117, 2010.
12. Yang, J., M. Huang, and J. Peng, "Directive emission obtained by Mu and epsilon-near-zero metamaterials," *Radioengineering Journal*, Vol. 18, 2009.
13. Tassin, P., X. Sahyoun, and I. Veretennicoff, "Miniaturization of photonic waveguides by the use of left-handed materials," *Appl. Phys. Lett.*, Vol. 92, 203111, 2008.
14. Oulton, R. F., V. J. Sorger, D. A. Genov, D. F. P. Pile, and X. Zhang, "A hybrid plasmonic waveguide for subwavelength confinement and long-range propagation," *Nature Photonics*, Vol. 2, 496–500, 2008.
15. Abdelaziz, A. F., T. M. Abuelfadl, and O. L. Elsayed, "Realization of composite right/left-handed transmission line using coupled lines," *Progress In Electromagnetics Research*, Vol. 92, 299–315, 2009.
16. Niu, J. X. and X. L. Zhou, "Analysis of balanced composite right/left handed structure based on different dimensions of complementary split ring resonators," *Progress In Electromagnetics Research*, Vol. 74, 341–351, 2007.
17. Caloz, C. and T. Itoh, *Electromagnetic Metamaterials: Transmission Line Theory and Microwave Applications*, John Wiley and

Sons, Inc., 2006.

18. Caloz, C. and T. Itoh, "Application of the transmission line theory of left-handed (LH) materials to the realization of a microstrip, 'LH line'," *IEEE Antennas and Propagation Society International Symposium*, Vol. 2, 412–415, Aug. 2002.
19. Wang, Y., Y. Zhang, H. Li, L. He, F. Liu, and H. Chen, "Coupling characteristics between composite right-/left-handed transmission line and conventional transmission line," *International Conference on Microwave and Millimeter Wave Technology, 2008. ICMMT 2008*, Vol. 4, 1620–1623, Apr. 2008.
20. Dong, Y. D. and T. Itoh, "Composite right/left-handed substrate integrated waveguide and half-mode substrate integrated waveguide," *IEEE MTT-S International Microwave Symposium Digest, 2009, MTT'09*, 49–52, Jun. 2009.
21. Hong, W., B. Liu, Y. Wang, Q. Lai, H. Tang, X. X. Yin, Y. D. Dong, Y. Zhang, and K. Wu, "Half mode substrate integrated waveguide: A new guided wave structure for microwave and millimeter wave application," *Proc. Joint 31st Int. Conf. Inf. Millim. Waves 14th Int. Conf. Terahertz Electron.*, 18–22, Shanghai, China, Sep. 2006.
22. Wang, Y., W. Hong, Y. Dong, B. Liu, H. J. Tang, J. Chen, X. Yin, and K. Wu "Half mode substrate integrated waveguide (HMSIW) bandpass filter," *IEEE Microwave and Wireless Components Letters*, Vol. 17, No. 4, 265–267, Apr. 2007.
23. Liu, B., W. Hong, Y. Q. Wang, Q. H. Lai, and K. Wu, "Half mode substrate integrated waveguide (HMSIW) 3-dB coupler," *IEEE Microwave and Wireless Components Letters*, Vol. 17, No. 1, 22–24, Jan. 2007.
24. Wang, Z., X. Li, S. Zhou, B. Yan, R. M. Xu, and W. Lin, "Half mode substrate integrated folded waveguide (HMSIFW) and partial h-plane bandpass filter," *Progress In Electromagnetics Research*, Vol. 101, 203–216, 2010.
25. Lai, Q. H., W. Hong, Z. Q. Kuai, Y. S. Zhang, and K. Wu, "Half-mode substrate integrated waveguide transverse slot array antennas," *IEEE Transactions on Antennas and Propagation*, Vol. 57, No. 4, 1064–1072, Apr. 2009.
26. Ansoft HFSS software, version 11.
27. Lubkowski, G., R. Schuhmann, and T. Weiland, "Extraction of effective metamaterial parameters by parameter fitting of dispersive models," *Microwave Optics and Technology Letters*, Vol. 49, No. 2, 285–288, Feb. 2007.

28. Marcuvitz, N., *Waveguide Handbook*, Peter Peregrinus Ltd., 1986.
29. Matthaei, G., L. Young, and E. M. T. Jones, *Microwave Filters, Impedance Matching Networks and Coupling Structures*, Artech House, 1980.
30. Liu, C. and K. Huang, "A compact substrate integrated waveguide band-pass filter," *PIERS Proceedings*, 1135–1138, Cambridge, USA, Jul. 5–8, 2010.
31. Deng, H., "A novel broad bandpass filter with coplanar resonators," *11th IEEE Singapore International Conference on Communication Systems, 2008, ICCS 2008*, 630–631, Nov. 2008.
32. Bornemann, J. and S. Y. Yu, "Circular waveguide TM_{11}-mode resonators and their application to polarization-preserving band-pass and quasi-highpass filters," *German Microwave Conference 2010*, 202–205, Mar. 2010.